Tight-binding model for exciton-polariton condensates in external potentials

Piotr Stępnicki and Michał Matuszewski
Instytut Fizyki PAN, Aleja Lotników 32/46, 02-668 Warsaw, Poland
(Received 13 May 2013; published 23 September 2013)

We propose a mean-field model to describe exciton-polariton condensates in deep periodic external potentials. We derive a set of coupled discrete equations for both condensed and uncondensed components, with interaction and tunneling coefficients obtained within the tight-binding approximation. We use the model to explain the intriguing phenomenon of increasing density modulation in a one-dimensional valley with disorder, reported by F. Manni *et al*. [Phys. Rev. Lett. **106**, 176401 (2011)].

DOI: 10.1103/PhysRevA.88.033626 PACS number(s): 03.75.Lm, 71.36.+c

I. INTRODUCTION

The experimental observation of Bose-Einstein condensates (BECs) of ultracold atoms [1] was a major breakthrough in physics, opening a new chapter in the studies of quantum systems. Recently, degenerate bosonic states have been achieved in semiconductor microcavities, in which photons are confined and strongly coupled to excitons [2]. The dressed state of the two, called the exciton-polariton, is a remarkable quasiparticle, characterized by an effective mass orders of magnitude smaller than the mass of the electron [3]. This property made condensation at room temperature possible [4]. At the same time, the coupling to photons allowed for direct observation of quantum phenomena such as superfluidity and quantum vortices [5].

Although the first exciton-polariton condensates were strongly trapped by the disorder present in the samples, the semiconductor technology makes it possible to fabricate sophisticated structures, such as micropillars, dots, or nanowires [6], which can provide a well-defined artificial potential for polaritons. Alternatively, the potential can be created through the deformation of the sample [7,8]. One of the simplest and yet nontrivial types of potentials is the periodic one, which mimics the structure of a crystal. While polariton condensation in deep periodic potentials has already been observed [8], appropriate theoretical models are still not well developed. Although the mean-field description with the generalized Gross-Pitaevskii equation (GPE) proved to be adequate to explain many experiments, it is instructive to consider approximate models, which may give better insight into the underlying physics. One of the successful theoretical models used, among others, in the context of nonlinear optics and BECs of ultracold atoms [9] is the tight-binding approximation, which leads to the discrete version of the GPE (or the discrete nonlinear Schrödinger equation, DNLSE). This equation can be thought of as a bridge between the two-mode Josephson model [10] and the continuous GPE. Importantly, it predicts many qualitatively distinct effects, such as discrete solitons and vortices [11], dispersion management [12], and soliton steering [13].

In this paper, we derive self-consistently a set of discrete equations to model the evolution of nonresonantly pumped condensate in a deep periodic potential. The model is based on the mean-field GPE description taking into account the densities of active and inactive reservoirs. We find that to model this dissipative system accurately, it is necessary to take into account several nontrivial terms that are absent in the conservative discrete GPE.

Furthermore, we use the properties of the model to explain the intriguing phenomenon, reported in [14]. The authors of that paper were investigating the density profile of a condensate placed in a one-dimensional potential valley with disorder. They found that with the increase of the pumping intensity, the spatial modulation of the density increased. This contradicts the picture where the nonlinear interactions introduce an effective screening of the disorder potential [8,15]. We find that the increase of the modulation could be related to the buildup of the π-phase difference between adjacent cells of the potential [16], which can be explained qualitatively within the tight-binding approximation.

II. MODEL

We start with a model of a nonresonantly pumped polariton condensate in a one-dimensional (1D) nanowire, consisting of a set of coupled equations for the complex polariton order parameter $\psi(\mathbf{r},t)$ and the densities of active and inactive reservoirs $n_{\mathrm{A}}(\mathbf{r},t)$, $n_{\mathrm{I}}(\mathbf{r},t)$ [17] (which include free carriers, excitons, and uncondensed polaritons),

$$i\frac{\partial\psi}{\partial t} = \left\{-\frac{\hbar\nabla^2}{2m^*} + g_{\mathrm{C}}|\psi|^2 + V(\mathbf{r}) + g_{\mathrm{R}}n_{\mathrm{A}} + g_{\mathrm{R}}n_{\mathrm{I}} - \frac{i}{2}\left(\gamma_c - R_{\mathrm{sc}}n_{\mathrm{A}}\right)\right\}\psi, \quad (1)$$

$$\frac{\partial n_{\mathrm{A}}}{dt} = -(\gamma_{\mathrm{A}} + R_{\mathrm{sc}}|\psi|^2)n_{\mathrm{A}} + \frac{1}{\tau_{\mathrm{R}}}n_{\mathrm{I}}, \quad (2)$$

$$\frac{\partial n_{\mathrm{I}}}{dt} = P(\mathbf{r},t) - \gamma_{\mathrm{I}}n_{\mathrm{I}} - \frac{1}{\tau_{\mathrm{R}}}n_{\mathrm{I}}, \quad (3)$$

where m^* is the effective mass of lower polaritons, $V(\mathbf{r})$ is the potential, R_{sc} is the rate of stimulated scattering, γ_c, γ_{A}, and γ_{I} are the polariton and reservoir loss rates (for active and inactive reservoirs, respectively), g_{C} and g_{R} are the respective interaction coefficients, and $P(\mathbf{r},t)$ is the exciton creation rate related to the pumping profile.

The one-dimensional version of Eqs. (1)–(3) can be derived by assuming a Gaussian transverse profile for $|\psi|^2$, n_{A}, and n_{I} in the y direction, i.e., $|\psi^{2\mathrm{D}}(x,y,t)|^2 = |\psi(x,t)|^2\phi(y)$, where $\phi(y) = \exp(-y^2/d^2)/(\pi d^2)^{1/4}$. In the one-dimensional case the nonlinear coefficients R_{sc}, g_{C}, and g_{R} are rescaled as

$(R_{\rm sc}, g_i) = (R_{\rm sc}^{\rm 2D}, g_i^{\rm 2D})/\sqrt{2\pi d^2}$, where d is the width of the transverse profile, comparable to the nanowire thickness.

We note that while the discretization method can be applied to the two-dimensional case, the effects discussed in Sec. III are related to the one-dimensional geometry of the system. Therefore, in the following we restrict our considerations to the one-dimensional case.

A. Derivation of the discrete equations

In the following, we assume that the potential $V(\mathbf{r})$ is deep enough that the polaritons are mostly localized in its well-defined minima but the tunneling between adjacent minima is not negligible. For simplicity, we consider the one-dimensional geometry with a periodic potential, but the derivation can be easily extended to the general case. According to our assumptions, the polariton wave function and reservoir densities can be written as

$$\begin{aligned} \psi(x,t) &= \sum_j \varphi(x - jL) c_j(t), \\ n_{\rm A}(x,t) &= \sum_j \eta_A(x - jL) n_{\rm A}^j(t), \\ n_{\rm I}(x,t) &= \sum_j \eta_I(x - jL) n_{\rm I}^j(t). \end{aligned} \tag{4}$$

The function $\varphi(x)$ is analogous to the *atomic orbital* function in the tight-binding approximation, and L is the spatial period of the potential $V(x)$. We note that the above assumption effectively restricts our considerations to the lowest-energy band of the potential [9]. Although the choice of $\varphi(x)$, $\eta_A(x)$, and $\eta_I(x)$ does not change the form of the resulting discrete equations, it can influence the accuracy of the model through the value of the coefficients present in the discrete equations. We have found that the following substitutions provide a good agreement with the continuous model:

$$\begin{aligned} \varphi(x) &= N_1 \,\mathrm{sech}\,(ax), \\ \eta_A(x) &= \begin{cases} N_2[1 - b\,\mathrm{sech}^2(ax)], & -\frac{1}{2}L < x < \frac{1}{2}L, \\ 0, \quad \text{otherwise}, \end{cases} \\ \eta_I(x) &= \begin{cases} \frac{1}{L}, & -\frac{1}{2}L < x < \frac{1}{2}L, \\ 0, \quad \text{otherwise}, \end{cases} \end{aligned} \tag{5}$$

where parameters were chosen as $a = 0.9 + 0.1i$ and $b = 0.1$ and N_1 and N_2 are normalization constants introduced to satisfy the conditions

$$\int_{-\infty}^{+\infty} |\varphi|^2\, dx = \int_{-\infty}^{+\infty} |\eta_A|\, dx = 1. \tag{6}$$

After insertion of (4) and (5) into (3) and (2) and performing integration over the interval $L_j = [-L/2 + jL, L/2 + jL]$, one gets two sets of equations enumerated by j:

$$\frac{dn_{\rm I}^j}{dt} = P_j - \gamma_{\rm I} n_{\rm I}^j - \frac{1}{\tau_{\rm R}} n_{\rm I}^j, \tag{7}$$

$$\frac{dn_{\rm A}^j}{dt} = -(\gamma_{\rm A} + |c_j|^2 R_{\rm sc}\alpha_0) n_{\rm A}^j + \frac{1}{\tau_{\rm R}} n_{\rm I}^j, \tag{8}$$

where $\alpha_i = \int \eta_A |\varphi_i|^2\, dx$, $\varphi_j(x) = \varphi(x - jL)$, and $P_j = \int_{L_j} P\, dx$. To obtain the equation for polaritons, Eqs. (4) are inserted into (1), and both sides of the equation are multiplied by ϕ_j^* and integrated over space. All expressions on the right side of the equation containing products of $\varphi_m \varphi_j^*$ such that $|j - m| > 1$ are omitted, as well as similar terms involving η_A or η_I and nonlocal polariton-polariton interaction terms. We checked that in numerical simulations, all these terms give a negligible contribution. Finally, we obtain the equation for polaritons in the form

$$\begin{aligned} i\frac{dc_j}{dt} &= Ac_j + B(c_{j+1} + c_{j-1}) + Cc_j|c_j|^2 \\ &\quad + n_{\rm A}^j\left(g_{\rm R} + i\frac{R_{\rm sc}}{2}\right)(\alpha_1 c_{j-1} + \alpha_0 c_j + \alpha_1 c_{j+1}) \\ &\quad + n_{\rm I}^j g_{\rm R}(\beta_1 c_{j-1} + \beta_0 c_j + \beta_1 c_{j+1}), \end{aligned} \tag{9}$$

where $\beta_i = \int \eta_I |\varphi_i|^2\, dx$ and

$$\begin{aligned} A &= \int \left(\frac{\hbar}{2m^*}|\nabla\varphi|^2 + V|\varphi|^2\right)dx - \frac{i}{2}\gamma_c, \\ B &= \int \left[\frac{\hbar}{2m^*}\nabla\varphi_{j-1}\nabla\varphi_j^* + \left(V + \frac{i}{2}\gamma_c\right)\varphi_j^*\varphi_{j-1}\right]dx, \\ C &= \int g_{\rm C}|\varphi|^4\, dx. \end{aligned}$$

The first three terms in Eq. (9) have a similar form as in the standard discrete nonlinear Schrödinger equation. However, it is important to note that while the coefficient C is real and positive, both A and B are complex in general. The last two terms in Eq. (9) represent the influence of reservoirs. We found that all of the terms in the above equation are important for a good quantitative agreement between the continuous and discrete models. Nevertheless, qualitative agreement could also be obtained when neglecting some of the terms, such as the secondary terms governing interaction with the reservoir, namely, $n_{\rm A}^j \alpha_1 c_{j\pm1}$ and $n_{\rm I}^j \beta_1 c_{j\pm1}$.

The advantage of using discrete models such as (7)–(9) instead of continuous models is clear from the point of view of the numerical efficiency. In the latter case, it is necessary to use many points of a numerical mesh for each spatial period of $V(x)$ to obtain reliable results. Moreover, in many situations the discretized models allow us to understand the underlying physical processes or obtain analytical solutions in a more straightforward way.

B. Stationary solutions

When looking for stationary states, the set of discrete equations (7), (8), and (9) can be reduced to one. By setting $dn_{\rm A}^j/dt = dn_{\rm I}^j/dt = 0$ and $c_j(x,t) = c_j^{(0)}(x)e^{-i\mu t}$ one gets

$$\begin{aligned} n_{\rm I}^j &= \frac{P_j}{\tau_{\rm R}^{-1} + \gamma_{\rm I}}, \\ n_{\rm A}^j &= \frac{P_j}{\tau_{\rm R}\gamma_{\rm I} + 1}\frac{1}{\alpha_0 R_{\rm sc}|c_j|^2 + \gamma_{\rm A}}, \\ c_j\mu &= Ac_j + B(c_{j+1} + c_{j-1}) + C|c_j|^2 c_j \\ &\quad + \frac{E}{|c_j|^2 + F}P_j(\alpha_0 c_j + \alpha_1 c_{j-1} + \alpha_1 c_{j+1}) \\ &\quad + DP_j(\beta_0 c_j + \beta_1 c_{j-1} + \beta_1 c_{j+1}), \end{aligned} \tag{10}$$

where

$$D = \frac{g_R}{\tau_R^{-1} + \gamma_I},$$
$$E = \alpha_0^{-1} \frac{\frac{g_R}{R_{sc}} + \frac{i}{2}}{\tau_R \gamma_I + 1},$$
$$F = \frac{\gamma_A}{\alpha_0 R_{sc}}.$$

While at low pumping the only stationary solution corresponds to zero polariton density, after crossing a certain critical value of pumping the zero solution becomes unstable and another stable solution appears. This solution corresponds to a finite mean-field polariton density with a well-defined phase, which indicates symmetry breaking and the formation of a polariton condensate.

To determine the threshold pumping intensity P_{th} it is necessary, in principle, to know the condensate spatial profile. In the simplest approximation we consider the homogeneous $P(x) = P_{th}$ and neglect the kinetic term. For such conditions it is straightforward to estimate P_{th} for both models. It turns out that this value works quite well also for inhomogeneous pumping profiles. The precise values of threshold pumping intensities for the parameters considered in the next section are described by the formula below, where the factor 1.1 comes from numerical adjustments in the case of the Gaussian pumping profile,

$$P \geqslant P_{th} = 1.1 \gamma_c \gamma_A \frac{\tau_R \gamma_I + 1}{R_{sc}},$$
$$P_j \geqslant P_{th}^d = \gamma_c \gamma_A \frac{\tau_R \gamma_I + 1}{\alpha_0 R_{sc}}. \quad (11)$$

The above suggests the scaling $P \approx \alpha_0 P_j$ when comparing results of the two models in the deeply modulated case. This is a natural choice since it takes into account both the fact that P_j is P integrated over space and the fact that the creation of polaritons is mediated by the reservoir.

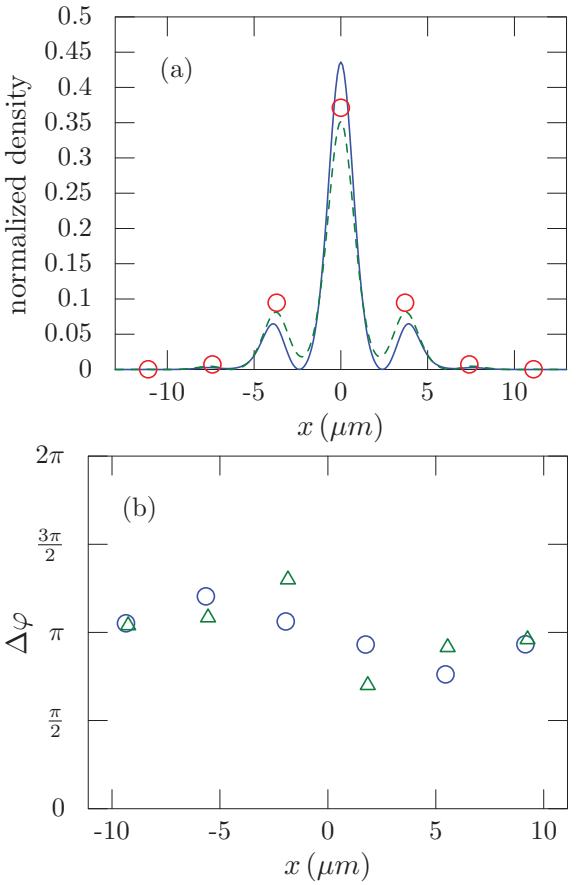

FIG. 1. (Color online) (a) Stationary polariton density $|\psi|^2$ as predicted by the discrete model (dashed line) and the continuous model (solid line). The open circles show the amplitude of the discrete function $|c_j|^2$. (b) Phase difference between adjacent cells for discrete (triangles) and continuous (circles) models. For the continuous model the phase was evaluated in the cell center. Here $P = 1.35 P_{th}$. All calculations were performed for $m^* = 10^{-4}\, m_e$, $g_C = 8.08 \times 10^{-4}\ \mu$m ps^{-1}, $g_R = 6.73 \times 10^{-5}\ \mu$m ps^{-1}, $R_{sc} = 6.73 \times 10^{-2}\ \mu$m ps^{-1}, $\tau_R = 6.58$ ps, $\gamma_A = 15.2$ ps^{-1}, $\gamma_I = 1.97 \times 10^{-3}$ ps^{-1}, $\gamma_c = 0.99$ ps^{-1}.

III. NUMERICAL RESULTS

In [14], peculiar density patterns were observed during condensation of polaritons in a quasi-one-dimensional valley potential. Due to the disorder in the sample, the density profile of the polariton condensate was modulated in the direction of the valley. Interestingly, above the threshold for condensation, the density modulation increased with the increase in pumping. At first sight, this appears to be a counterintuitive result since the effect of strong polariton-polariton interactions should lead to the screening of the built-in potential [8,15]. We argue that the density profile is highly modulated due the buildup of a phase difference between neighboring potential wells (see Sec. IV) and the lack of modulation for small pumping intensity ($P \sim P_{th}$) is an effect of emission from the noncondensed fraction of polaritons.

Although the experimental potential in [14] was due to disorder in the CdTe microcavity, we show that qualitatively similar results can be obtained in the case of a periodic potential. We assume that the periodic potential along the nanowire is of the form $V(x) = -V_0 \cos(2\pi x/L)$, where the spatial period is $L = 3.7\ \mu$m an $V_0 = 0.65$ ps^{-1} (the potential amplitude was chosen to be of the same order as the quadratic term $|\psi|^2 g_C$). The system is pumped with a Gaussian intensity profile, $P(x) = Pe^{-\frac{x^2}{2W}}$, where the profile half width $W = 5\ \mu$m is similar to the experimental value.

The results of simulations within the continuous and discrete models are shown in Figs. 1 and 2 for two different values of pumping P. The top panels show profiles of polariton condensate density in the stationary state, after a sufficiently long time for the evolution necessary for the stabilization of profiles. In the bottom panels we plot the difference in the phase of the condensate wave function between adjacent cells. Certainly, at these values of pumping, there is no effect of potential screening induced by the interactions. To the contrary, the density modulation remains high. This effect is explained by the phase profile of the condensate (bottom panels). For pumping intensity up to $1.4 P_{th}$ the phase between adjacent cells is approximately equal to π. Indeed, such configuration must lead to strong modulations of the density

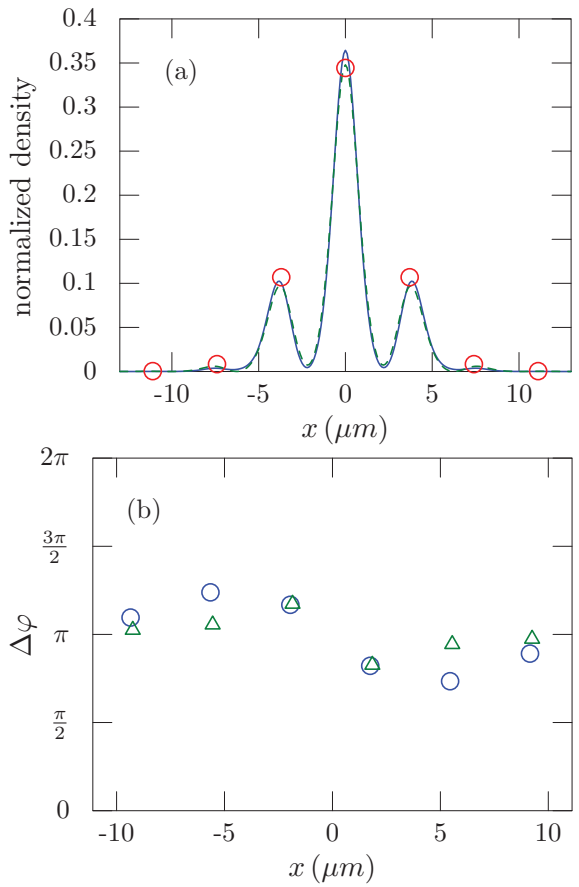

FIG. 2. (Color online) Same as in Fig. 1, but for $P = 1.1P_{\text{th}}$.

profile since the wave function $\psi(x)$ passes close to zero when traversing from one cell to another.

The results of the discrete model are in very good agreement with the continuous one for pumping intensity from $P < 1.4P_{\text{th}}$. We found that in the range $1.4P_{\text{th}} < P < 1.5P_{\text{th}}$ one cannot find a stationary solution, but instead there is a solution that develops some oscillations in time. The appearance of these oscillations results in a poorer agreement between the continuous and discrete models, although the two continue to agree qualitatively. At higher pumping $1.5P_{\text{th}} < P < 2.4P_{\text{th}}$ we observe a stationary state with the two side peaks being almost the same height as the central one (while the density is still strongly modulated) and a phase difference between the peaks roughly equal to 0.4π. While from experimental data one cannot judge if there are any oscillatory states, our simulations reproduce the general behavior of changes in the average density distribution.

For a more quantitative comparison with the experiment, we calculated the difference of the density profile with the reference profile. The formula used for the calculation is defined as [14]

$$\Delta\eta = \sqrt{\frac{1}{X}\int_X \left(\frac{\bar{\rho}(x) - \bar{\rho}_0(x)}{\bar{\rho}_0(x)}\right)^2}, \tag{12}$$

where X is the interval from -8 to 8 μm, $\rho(x)$ is the normalized sum of densities of the polariton condensate and

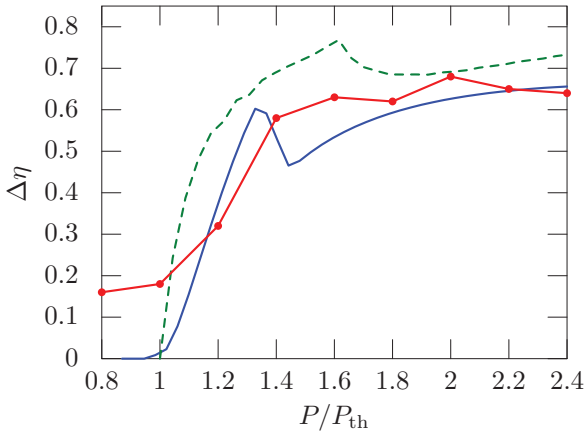

FIG. 3. (Color online) The contrast of the polariton density profile ψ calculated from (12). The red line with points is the experimental result of [14], and the solid blue line is the result of the continuous model. The dotted green line corresponds to the discrete model, where we replaced the integral by a sum in (12).

the noncondensed fraction,

$$\rho(x) = \frac{|\psi(x)|^2 + \rho_{\text{thermal}}(x)}{\sqrt{\int_X |\psi|^2 + \rho_{\text{thermal}}(x)dx}}, \tag{13}$$

and $\bar{\rho}(x)$ is the time average of $\rho(x)$. The reference profile $\bar{\rho}_0(x)$ is taken as the normalized profile $\bar{\rho}(x)$ at $P = P_{\text{th}}$. We assume that the density of the noncondensed fraction of polaritons is proportional to the density of the active reservoir $\rho_{\text{thermal}} = cn_{\text{A}}$. The value of c was chosen in such a way that the density of the thermal component is comparable to the density of condensed polaritons close to the threshold $P \approx P_{\text{th}}$.

The addition of ρ_{thermal} may seem artificial; however, one has to remember that the GPE cannot be used to model the behavior of polaritons before condensation, so to include the thermal fraction in the model one has to extend it. The addition of cn_{A} is negligible for any solution obtained for $P > P_{\text{th}}$, as it only affects the density profile for $P \leqslant P_{\text{th}}$, making the modulation less visible.

A similar formula was used in [14] to measure the "contrast" of the density profile. In Fig. 3 we show $\Delta\eta$ as a function of P_0, as calculated within the continuous and discrete models, and compare it with the results of [14]. However, one must be aware of the fact that the definition of contrast is not flawless and cannot be used as the only indication of agreement between theory and experiment.

Close inspection of density profiles in [14] reveals that the potential could be approximated to some extent by the periodic one. To support the validity of our calculation based on the periodic potential, we include a comparison with the results obtained in the case of a disorder potential (Fig. 4) for the same model. The disorder potential was obtained by taking a convolution of a random function and the Gaussian function to smooth out the disorder and set its spatial correlation length to be of the same order as in the experiment (several microns). Note that this procedure is equivalent to filtering out short-wavelength modes in $V(x)$. The density profiles for the

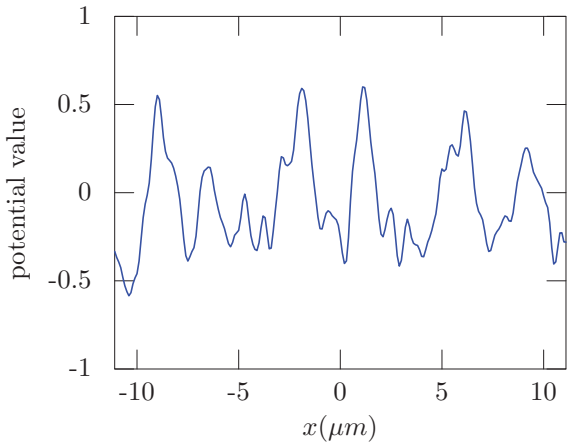

FIG. 4. (Color online) Disordered potential used for calculating polariton densities in Fig. 5.

disorder potential are displayed in Fig. 5. We can see that the same qualitative features are present in this case.

IV. BUILDUP OF THE π-PHASE DIFFERENCE

The effect of the spontaneous buildup of the approximate π-phase difference between adjacent cells is related to the appearance of the π state in recent experiments in shallow periodic potentials [16]. This effect was attributed to the creation of a metastable state in an effective "trap" for polaritons in the second energy band. The polaritons were able to overcome the effective bottleneck and relax to the ground state only at sufficiently high pumping intensity. Here we show that in the case of a deep potential, even in the absence of energy relaxation within the condensate, this effect may also be induced by the repulsive interactions between polaritons.

Within the discrete model, the effect can be understood by considering the transformation which relates solutions of discrete equations with attractive and repulsive interactions [18]. In the case of moderate pumping above threshold, when neglecting higher-order terms in Eq. (10), there is a one-to-one correspondence between solutions with positive and negative g_C due to the transformation:

$$\begin{aligned} c_j' &= (-1)^j c_j, \\ C' &= -C, \\ \mu' &= -\mu + 2[A + P_j(\alpha_0 E/F + \beta_0 D)]. \end{aligned} \tag{14}$$

Let us consider a large system with $P_j(x)$ slowly varying in space. In the case of attractive interactions, in both the presence and absence of the periodic potential, the system would have the tendency to decrease the variations of the phase in order to increase the magnitude of the negative interaction energy and decrease the kinetic energy contribution. The small variations of phase could only be induced by nonconservative terms, which correspond to the flux of the polariton density. By using the transformation (14) we can then conclude that in the case of repulsive interactions (and deep periodic potential), the preferred state will be the one where adjacent cells have approximately a π-phase difference. In the opposite case, that is, when only a single potential well is pumped ($P_j = 0$ for $j \neq 0$), we can again use the discrete model to obtain some general conclusions from an analytical solution. For all points except $j = 0$, Eq. (10) reads

$$c_j \mu = A c_j + B(c_{j+1} + c_{j-1}) + C|c_j|^2 c_j, \quad j \neq 0. \tag{15}$$

Away from the pumping spot, where the nonlinear term $C|c_j|^2 c_j$ can be omitted, we have the solution

$$c_j = c_0 \exp(-\kappa |j|), \tag{16}$$

where $\mathrm{Re}(\kappa) > 0$. Further on, we assume that Eq. (15) is valid for all points except $j = 0$. The relation between μ and κ is

$$\cosh(\kappa) = \frac{\mu - A}{2B}. \tag{17}$$

For convenience let us introduce variables r and ϕ such that $re^{i\phi} = e^{-\kappa}$. It is possible to obtain an equation that connects the phase difference between adjacent cells ϕ and the amplitude ratio denoted by $r < 1$. After multiplying by $2B$ and taking the imaginary part of both sides of Eq. (17),

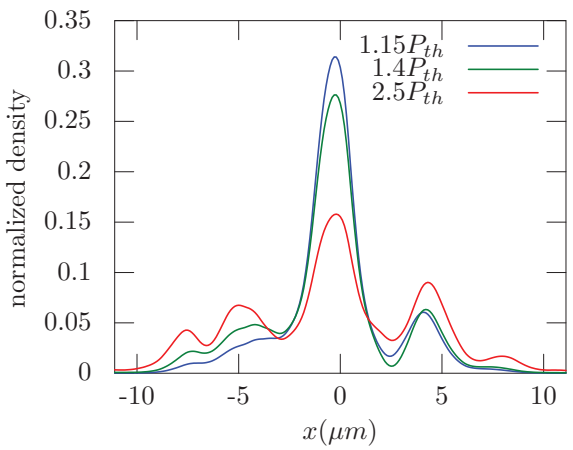

FIG. 5. (Color online) Normalized polariton density in the disordered potential at different pumping intensities.

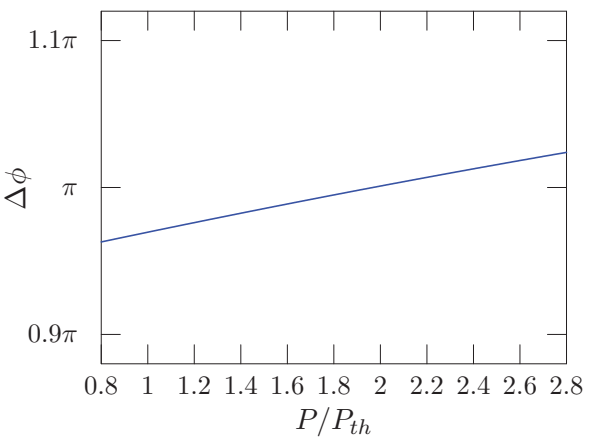

FIG. 6. (Color online) Phase difference between adjacent cells vs the pumping intensity p, from Eq. (16).

one gets

$$r(\phi) = \frac{-\frac{\mathrm{Im}A}{2|B|} \pm \sqrt{\left(\frac{\mathrm{Im}A}{2|B|}\right)^2 + \cos(\phi_B)^2 - \cos(\phi)^2}}{\sin(\phi + \phi_B)}, \quad (18)$$

where $\phi_B = \arg(B)$. It is easy to notice that r is real and positive for $\phi \in [\phi_B, \pi + \phi_B]$. Further calculations show that only one solution (with the minus sign) can be realized, as the positive solution results in $r > 1$ for every ϕ.

To determine r and ϕ as a function of P_j we resort to numerical solutions. Figure 6 shows the result for the parameters used in Figs. 1 and 2. Clearly, the phase difference ϕ is close to π for all realizable values of pumping.

This conclusion can be obtained in a straightforward way in the case of strong localization (strong pumping), where the nonlinear term dominates in the central spot and the amplitude decays quickly when moving away from the pumping spot. In this case, Eq. (17) becomes $\exp(\kappa) = \mu/B$. If the losses γ_c are modest, $\mathrm{Re}(B)$ must be approximately a negative real number for correspondence with Eq. (1). Hence, we again obtain $\phi = \arg(\mu/B) \approx \pi$.

V. CONCLUSIONS

In conclusion, we introduced a self-consistent mean-field model to describe the exciton-polariton condensates in deep periodic external potentials in the case of nonresonant pumping. We derived a set of coupled discrete equations for both condensed and uncondensed components, with interaction and tunneling coefficients obtained within the tight-binding approximation. Furthermore, by analyzing stationary solutions of the model, we explained the intriguing phenomenon of increasing density modulation in a one-dimensional valley with disorder observed in a CdTe microcavity. We pointed out that it is related to the spontaneous buildup of the π-phase difference between adjacent potential wells in the case of repulsive polariton interaction.

ACKNOWLEDGMENTS

We thank Barbara Piętka for useful discussions. This work was supported by National Science Center Grant No. DEC-2011/01/D/ST3/00482.

[1] M. H. Anderson, J. R. Ensher, M. R. Matthews, C. E. Wieman, and E. Cornell, Science **269**, 198 (1995); C. C. Bradley, C. A. Sackett, J. J. Tollett, and R. G. Hulet, Phys. Rev. Lett. **75**, 1687 (1995); K. B. Davis, M. O. Mewes, M. R. Andrews, N. J. van Druten, D. S. Durfee, D. M. Kurn, and W. Ketterle, *ibid.* **75**, 3969 (1995).

[2] J. Kasprzak, M. Richard, S. Kundermann, A. Baas, P. Jeambrun, J. M. J. Keeling, F. M. Marchetti, M. H. Szymańska, R. André, J. L. Staehli, V. Savona, P. B. Littlewood, B. Deveaud, and L. S. Dang, Nature (London) **443**, 409 (2006).

[3] A. V. Kavokin, J. J. Baumberg, G. Malpuech, and F. P. Laussy, *Microcavities* (Oxford University Press, Oxford, 2007).

[4] S. Christopoulos, G. Baldassarri Hoger von Högersthal, A. Grundy, P. G. Lagoudakis, A. V. Kavokin, J. J. Baumberg, G. Christmann, R. Butté, E. Feltin, J.-F. Carlin, and N. Grandjean, Phys. Rev. Lett. **98**, 126405 (2007).

[5] A. Amo, J. Lefrère, S. Pigeon, C. Adrados, C. Ciuti, I. Carusotto, R. Houdré, E. Giacobino, and A. Bramati, Nat. Phys. **5**, 805 (2009); K. G. Lagoudakis, M. Wouters, M. Richard, A. Baas, I. Carusotto, R. André, Le Si Dang, and B. Deveaud-Plédran, *ibid.* **4**, 706 (2008); H. Deng, H. Haug, and Y. Yamamoto, Rev. Mod. Phys. **82**, 1489 (2010).

[6] D. Bajoni, P. Senellart, E. Wertz, I. Sagnes, A. Miard, A. Lemaître, and J. Bloch, Phys. Rev. Lett. **100**, 047401 (2008); M. Galbiati *et al.*, *ibid.* **108**, 126403 (2012); E. Wertz, L. Ferrier, D. D. Solnyshkov, R. Johne, D. Sanvitto, A. Lemaître, I. Sagnes, R. Grousson, A. V. Kavokin, P. Senellart, G. Malpuech, and J. Bloch, Nat. Phys. **6**, 860 (2010).

[7] R. B. Balili, D. W. Snoke, L. Pfeiffer, and K. West, Science **316**, 1007 (2007).

[8] E. A. Cerda-Méndez, D. N. Krizhanovskii, M. Wouters, R. Bradley, K. Biermann, K. Guda, R. Hey, P. V. Santos, D. Sarkar, and M. S. Skolnick, Phys. Rev. Lett. **105**, 116402 (2010).

[9] P. G. Kevrekidis, *The Discrete Nonlinear Schrödinger Equation: Mathematical Analysis, Numerical Computations and Physical Perspectives* (Springer, Berlin, 2009); A. Trombettoni and A. Smerzi, Phys. Rev. Lett. **86**, 2353 (2001); O. Morsch and M. Oberthaler, Rev. Mod. Phys. **78**, 179 (2006).

[10] K. G. Lagoudakis, B. Pietka, M. Wouters, R. André, and B. Deveaud-Plédran, Phys. Rev. Lett. **105**, 120403 (2010); M. Abbarchi, A. Amo, V. G. Sala, D. D. Solnyshkov, H. Flayac, L. Ferrier, I. Sagnes, E. Galopin, A. Lemaitre, G. Malpuech, and J. Bloch, Nat. Phys. **9**, 275 (2013).

[11] D. N. Christodoulides and R. I. Joseph, Opt. Lett. **13**, 794 (1988); H. S. Eisenberg, Y. Silberberg, R. Morandotti, A. R. Boyd, and J. S. Aitchison, Phys. Rev. Lett. **81**, 3383 (1998); J. W. Fleischer, M. Segev, N. K. Efremidis, and D. N. Christodoulides, Nature (London) **422**, 147 (2003); B. A. Malomed and P. G. Kevrekidis, Phys. Rev. E **64**, 026601 (2001); D. N. Neshev, T. J. Alexander, E. A. Ostrovskaya, Y. S. Kivshar, H. Martin, I. Makasyuk, and Z. Chen, Phys. Rev. Lett. **92**, 123903 (2004); M. Matuszewski, C. R. Rosberg, D. N. Neshev, A. A. Sukhorukov, A. Mitchell, M. Trippenbach, M. W. Austin, W. Królikowski, and Y. S. Kivshar, Opt. Express **14**, 254 (2006).

[12] H. S. Eisenberg, Y. Silberberg, R. Morandotti, and J. S. Aitchison, Phys. Rev. Lett. **85**, 1863 (2000); M. Matuszewski, I. L. Garanovich, and A. A. Sukhorukov, Phys. Rev. A **81**, 043833 (2010).

[13] R. Morandotti, U. Peschel, J. S. Aitchison, H. S. Eisenberg, and Y. Silberberg, Phys. Rev. Lett. **83**, 2726 (1999).

[14] F. Manni, K. G. Lagoudakis, B. Pietka, L. Fontanesi, M. Wouters, V. Savona, R. Andre, and B. Deveaud-Plédran, Phys. Rev. Lett. **106**, 176401 (2011).

[15] G. Malpuech, D. D. Solnyshkov, H. Ouerdane, M. M. Glazov, and I. Shelykh, Phys. Rev. Lett. **98**, 206402 (2007).

[16] C. W. Lai, N. Y. Kim, S. Utsunomiya, G. Roumpos, H. Deng, M. D. Fraser, T. Byrnes, P. Recher, N. Kumada, T. Fujisawa, and Y. Yamamoto, Nature (London) **450**, 529 (2007).

[17] K. G. Lagoudakis, F. Manni, B. Pietka, M. Wouters, T. C. H. Liew, V. Savona, A. V. Kavokin, R. André, and B. Deveaud-Plédran, Phys. Rev. Lett. **106**, 115301 (2011).

[18] Y. S. Kivshar, Opt. Lett. **18**, 1147 (1993).